Proceedings of the 17th Pan-American Conference on Soil Mechanics and Geotechnical Engineering (XVII PCSMGE), and 2nd Latin-American Regional Conference of the International Association for Engineering Geology and the Environment (IAEG), La Serena Chile, 2024.

Stabilization of Saladillo Waterfall, Rosario, Santa Fe, Argentina. Geotechnical & Structural solution for the retrogressive erosion problem.

Estabilización de la Cascada Saladillo, Rosario, Santa Fe. Solución geotécnica & estructural al problema de la erosión retrogresiva.

Jorge G. Laiun & Pedro Fernandez
SRK Consulting Argentina, jlaiun@srk.com.ar, pfernandez@srk.com.ar

Virginia Sosa
Universidad Nacional de Rosario, FCEIA, Rosario, Argentina, virsosa@fceia.unr.edu.ar

ABSTRACT: The Saladillo Stream serves as a physical boundary, separating the city of Rosario from Villa Gobernador Galvez in Santa Fe, Argentina. It has a plain topography with geological and hydraulic conditions that result in complex processes of non-stabilized regressive erosion with block fall, giving rise in its final stretch towards the Paraná River to the so-called *Cascada del Saladillo* (Saladillo Falls). This is a natural horseshoe-shaped waterfall that has a height of ~15 m and a width of 64 m at the base, composed of silts and clays over-consolidated with natural calcareous cementation on a thick layer of dense to very dense sands. To stop the receding process of the waterfall and prevent the destruction of a major road bridge with infrastructure services, a retaining structure was initially designed using diaphragm walls in combination with jet grouting and was subsequently updated to a retaining wall linked by beams to diaphragm walls modules to meet the project schedule. This paper describes the tender project for the initial solution and the geotechnical campaign carried out; moreover, it presents details of the updated the technical solution including the geotechnical-structural FEM2D and FEM3D analyses carried out for the design of an atypical structure with few records available worldwide.

KEYWORDS: waterfall, regressive erosion, rigid double diaphragm walls frame, numerical model.

1 INTRODUCTION

The Saladillo stream features, in its final stretch towards the Paraná River, a natural horseshoe-shaped waterfall called *Cascada del Saladillo* with a drop of approximately fifteen meters and a base width of sixty-five meters. Its geological conformation and hydraulic conditions give rise to complex processes of regressive hydraulic erosion, which have necessitated numerous projects and temporary solutions over the years (Figure 1).

Figure 1. Saladillo waterfall and the Molino Blanco bridge, April 2017.

This mechanism involves the removal of material from the base due to the impact of the falling jet, forming a sinkhole that extends both downstream and upstream. In the latter case, when the base of the waterfall front is eroded, a soil cantilever forms and breaks under its own weight. The removed material moves downstream, and deposits or banks may form, which are then exposed to the water.

Cascada del Saladillo has the particularity of still not being stabilized; it has receded by more than 1700 m over the past 70 years and is currently less than 200 m away from Molino Blanco bridge. This structure connects the cities of Rosario with Villa Gobernador Galvez in the province of Santa Fe, and it includes a section with a gas pipeline, fiber optic conduit and other services. The 50-year recurrent flood has a peak flow of 1250 m^3/s, but the processes of failure and retreat of the waterfall usually occur when the stream experiences events of varying durations with flow rates above 400/500 m^3/s (Figure 2).

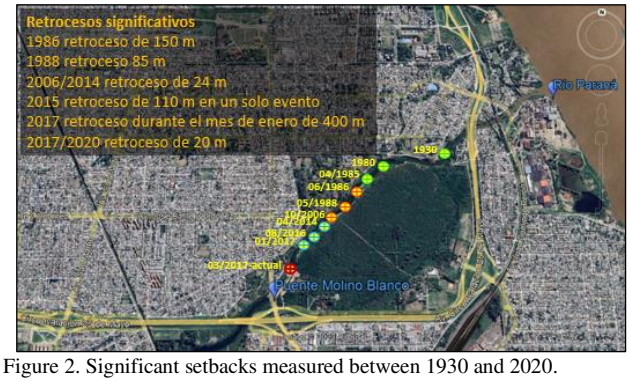

Figure 2. Significant setbacks measured between 1930 and 2020.

The Saladillo stream basin is classified as exorheic and follows the typology of a plain course with a meandering pattern. It is in the southeast of the province of Santa Fe and covers an area of approximately 3,145 km². Its main course is 145 km long, running from W-SE to E-NE with an average gradient of 0.57 m/km. The approximate coordinates of the stream at its headwaters are 33° 40' south and 61° 43' west, and at its mouth 32° 59' south and 60° 36' west (Figure 3).

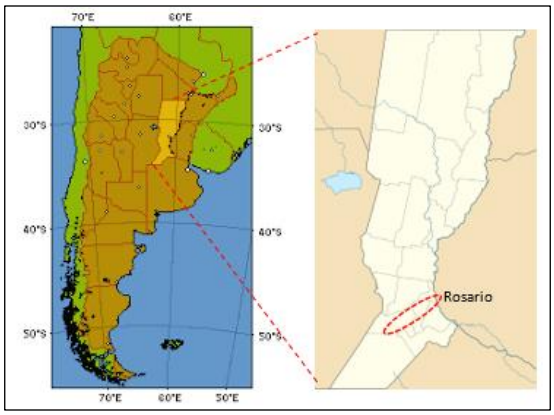

Figure 3. Geographical location of A° Saladillo in the province of Santa Fe, Argentina.

The area encompassed by the basin in its upper section is primarily agricultural, while its final section crosses the largest urban centers in the province. These aspects are emphasized due to their significant impact on changes in runoff caused by canalizations and the attention required for their consequences on the watercourse and soils of the floodplain throughout the basin.

2 RIVERBED EROSION PHENOMENA

Riverbed erosion is analyzed using the one-dimensional morphodynamic model known as ERCAS. This model simulates the main processes governing the retrograding time evolution of the massive cascade collapse mechanism in cohesive soils due to geotechnical instability associated with bracket failure. The model enables the estimation of effective bed erosion at the foot of the cascade and the impact of base scour caused by the counterclockwise backward vortex (Figure 4). Basile and Riccardi provide the calibration and validation of this model for the Saladillo waterfall (Basile, 2017).

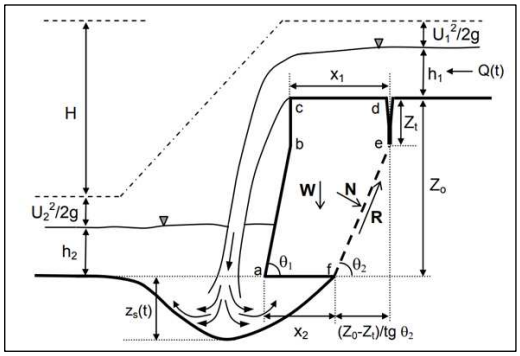

Figure 4. Bed erosion phenomena. Basile and Riccardi (2017).

This model was calibrated and validated using six floods observed in the Saladillo stream, with error ranges from 9% to 12%. These observations considered peak flows per unit width between 6 m^3/s and 12 m^3/s. Under these conditions, the maximum equilibrium erosion depth during a flood and for a fixed cascade can be estimated from Eq. 1.

$$Z_{se\,P} = 1.755\, q_p^{0.5198}\, V_h^{0.0614}\, H_p^{0.1411} - h_{2p} \qquad (1)$$

Where, q_p is the peak flow specified in $[m^2/s]$, V_h is the volume of the hydrograph in $[hm^3]$, H_p is the energy difference associated with the peak flow in $[m]$ and h_{2p} is the undisturbed depth downstream of the jump for q_p in $[m]$.

During a flood, this equilibrium erosion is achieved only if the duration is long enough for the erosion pool to reach a state of regime or equilibrium. If the bed sediment is non-cohesive (sands), this may occur even for floods of short duration. However, in consolidated cohesive beds and short-duration floods, common in streams in southern Santa Fe (such as Saladillo), achieving this erosion is unlikely; in other words, the effective erosion depth is limited by the duration of each flow that composes the hydrograph and is less than the equilibrium depth (Basile, 2017). Nonetheless, given the presence of sandy strata, it is considered in the design of this support work that the flood duration (peak flow) is sufficient for the maximum equilibrium erosion depth to be reached.

Figure 5 illustrates the erosion level as a function of the peak flow and the return period associated with each flow. For the geotechnical design of this project, a return period equal to 100 years was considered. This corresponds to a peak flow equal to 1500 m^3/s and an erosion level of -4.0 m. For verification purposes only, the structure's behavior was also evaluated up to a maximum erosion level of -7.0 m in the center of the channel.

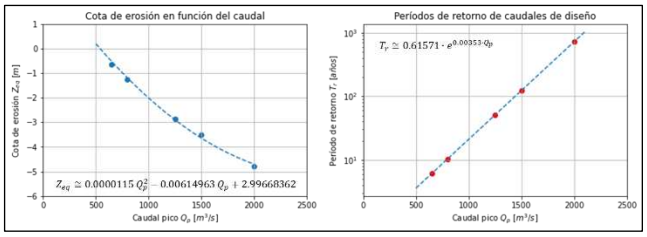

Figure 5. Erosion level, return period and river flow.

3 SITE DESCRIPTION

3.1 *Geological and Geotechnical description*

The Saladillo stream, a tributary of the Paraná River, is classified as a plain course with meandering development. It was once a temporary watercourse or drainage of the great plain with a slope towards the Paraná River, which later expanded and took on a meandering shape up to its mouth.

The site under study belongs to the geological province known as the *Llanura Chacho - Bonaerense*, which dates to the Quaternary period. The sediments studied correspond to the *Llanura Pampeana* sedimentary basin, specifically the *Rosario morphostructural sub-basin*, which describes an arc bordered to the east by the Paraná River and includes an area enclosed by the

southeastern end of the province of Santa Fe and part of the northeastern section of the province of Buenos Aires (Sosa V., 2012). Figure 6 shows the location of the different sedimentary basins of the Pampean plain (Yrigoyen M., 1975).

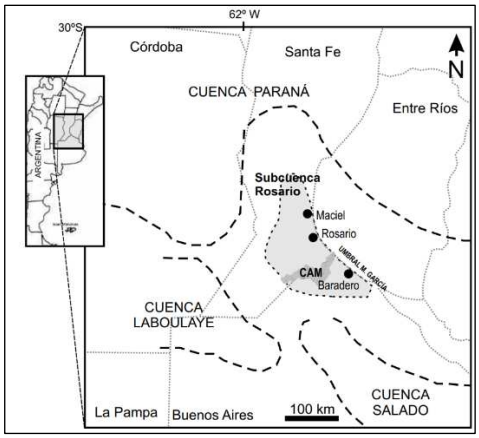

Figure 6. Sedimentary basins of the Pampean Plain (Yrigoyen M., 1975).

The geology of the Rosario sub-basin has been studied by the Institute of Physiography of the Faculty of Exact Sciences and Surveying (FCEIA) at the University of Rosario (UNR). There are four geotechnical units of interest in the area where the work will be carried out:

1. Saladillo Fm.: consists of silts, fine sandy silts, clays, and brown marl (*toscas*), with a dominant loessic character and colors ranging from light yellow to reddish-brown (Parent et al. 2010).
2. Ensenadense Fm.: transitional soils exist between the fine soils of the Saladillo Fm. and the clean sands of the Puelche Fm. These soils are composed of fine, yellowish to reddish-brown, laminated sands. At the base, there are alternating lenses of green-colored lacustrine clay, sometimes slightly loamy (Parent et al. 2010).
3. Puelche Fm.: composed of dense sands, these sands range from poorly to well graded, with an average particle size that increases with depth. They are uncemented, with low fines content, and of fluvial origin (Parent et al., 2010). The base of the Puelche Fm. is characterized by silt-clay layers with a significant proportion of sandy and gravelly fraction, as well as some gravels.
4. Paraná Fm.: composed of green clays with high plasticity and low silt content.

3.2 *Geotechnical causes of the waterfall,*

A sector of the Pampean plain in the province of Santa Fe was fractured into a succession of tectonic blocks parallel to each other, which moved differentially, creating the current morphology of narrow and elongated tectonic blocks. This process formed five hydrographic basins corresponding to the San Lorenzo, Ludueña, Saladillo Frias and Seco streams (Pasotti, 1982). One of these faults (highlighted in yellow) led to the formation of the waterfalls in the Saladillo stream (highlighted in red) and the Pavón stream (Figure 7).

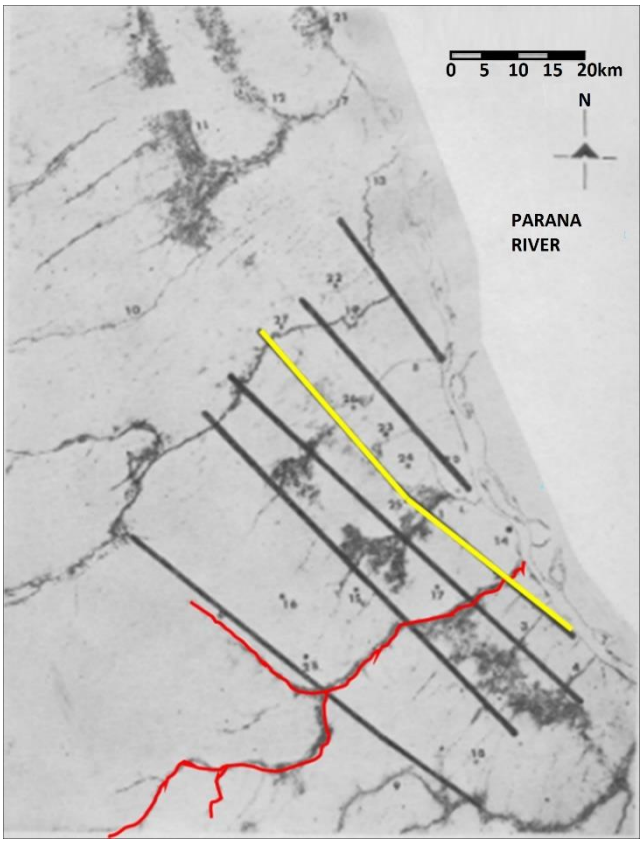

Figure 7. View of the 6 faults. Saladillo stream (red) and the geological fault (yellow) (based on Pasotti, 1982).

In terms of hydro-meteorological behavior, the region experiences well-defined seasons, characterized by excess rainfall from late summer to early autumn and precipitation deficits from late spring to midsummer.

3.3 *Geotechnical profile*

Figure 8 shows the location of the boreholes conducted in 2022. Figure 9 presents the interpreted stratigraphic profile, referencing elevation from the IGN (National Geographic Institute).

The soil classification according to Unified Soil Classification System (USCS) for each identified soil layer is provided below:

- A: CL, ML, CH. firm to very firm consistency, variable plasticity, preconsolidated. Saladillo Fm.
- B: ML. hard to very hard consistency, strongly cemented erratic soil, low plasticity, highly preconsolidated. Saladillo Fm.
- C: MH, CL, ML. very firm or hard consistency, higher plasticity than B, preconsolidated. Saladillo Fm.
- D: SM. very dense relative density, ferruginous spots, no plastic. Ensenadense Fm.
- E: CL, CH, ML. very hard consistency, variable plasticity, erratic lens, preconsolidated. Ensenadense Fm.
- F: SM. very dense relative density, no plastic. Puelche Fm.

Figure 8. Location of geotechnical borings.

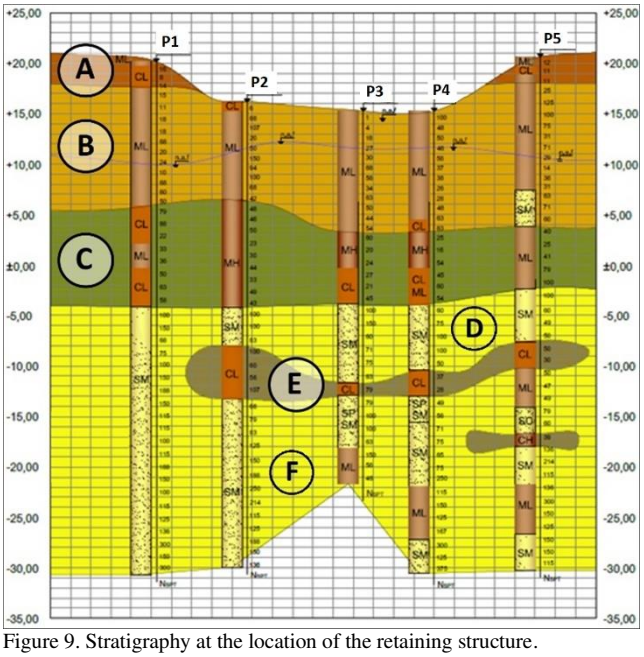

Figure 9. Stratigraphy at the location of the retaining structure.

3.4 *Constitutive model calibration*

The HSM model (Hardening Soil Model - Isotropic Hardening) included in the Plaxis software (Schanz, T., 1998) was utilized for geotechnical analysis. This is an isotropic hardening model for materials undergoing plastic compression and shear deformation for cyclic and static loads. The model correctly allows the increase in stiffness and strength with confining pressure and the hardening before failure with a hyperbolic stress-strain response (Kondner, R.L., 1963).

Table 1 presents a summary of the geotechnical parameters adopted for each of the strata involved in the reference problem, according to the HSM model.

To validate the geotechnical parameters, triaxial tests simulation were performed and compared with laboratory results. The Plaxis 2D SoilTest tool was used for the simulations, considering drained and undrained triaxial tests as appropriate and utilizing the Hardening Soil Model (HSM).

Table 1. Soil parameters for HSM constitutive model for each soil layer.

Parameter	*A*	*B*	*C*	*D/F*	*E*
Specific Gravity (kN/m^3)	19	19	18.5	20	19.5
Angle of Friction (deg)	31	33	28	36	29
Effective Cohesion (kPa)	15	30	20	0	25
Dilatancy (deg)	0	0	0	0	0
Ref. Pressure (kPa)	100	100	100	100	100
Ref. Stiffness 50% (MPa)	50	100	70	105	70
Ref. Stiffness Oed. (MPa)	50	100	70	105	70
Ref. Stiffness reloading (MPa)	120	250	170	260	175
Stress Exponent	0.40	0.40	0.40	0.55	0.40
Poisson's Ratio	0.25	0.25	0.25	0.25	0.25
Permeability (m/day)	1.0	1.0	0.1	30	0.1
Interface Reduction	0.70	0.70	0.70	0.70	0.70
Coefficient K_0	0.60	0.75	0.65	0.45	0.60
Preconsolidation Pressure (kPa)	650	1350	1100	350	1100

Figure 10 presents the effective stress trajectories (p'-q diagram) of undrained triaxial tests on samples from layers B and C, respectively. The solid line shows the experimental results, while the dotted line represents the trajectories obtained from the simulations. The adopted stiffness is higher than that in the triaxial test to compensate for alteration in the cemented samples. The black dotted line represents the critical state failure envelope at constant volume, corresponding to the adopted parameters.

Figure 11 presents the effective deviatoric stress versus specific axial deformation ($p' - \epsilon_a$ diagram) of drained triaxial tests on samples of layers D and F. The samples were tested in the laboratory at two relative densities: 50% and 80%. The calibration was adjusted to represent average values of the samples at $\epsilon_a =$ 2%. A refinement of the calibration could show the friction angles for layers D and F as 34.5° and 37.5°, respectively. However, due to the limited number of tests performed and the inability to detect changes in layers when layer E is absent, the same set of parameters for both layers D and F was adopted for design considerations.

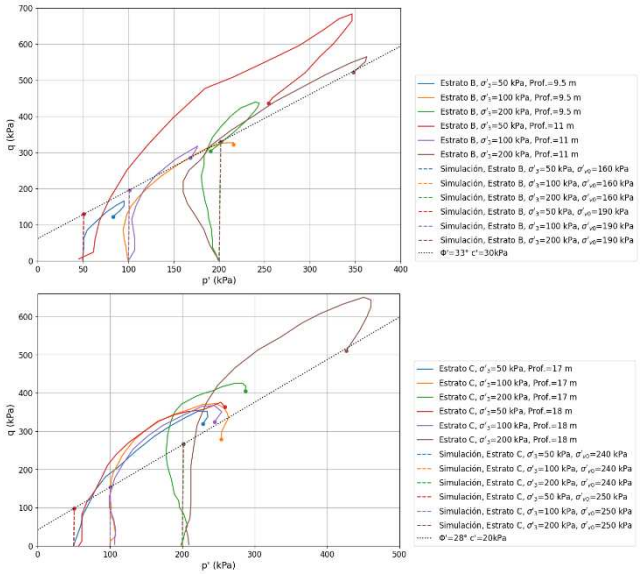

Figure 10. Effective stress trajectories (p'-q diagram) of undrained triaxial test and simulation for soil strata B and C.

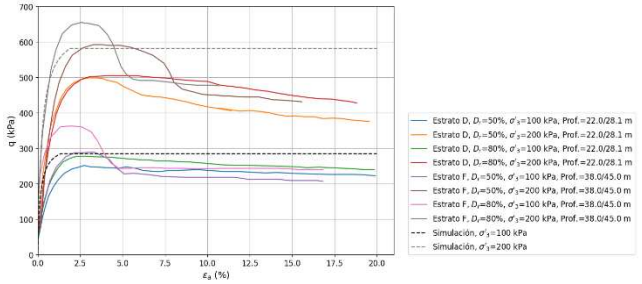

Figure 11. Effective deviatoric stress vs specific axial deformation ($p' - \epsilon_a$ diagram) of drained triaxial test and simulation for soil strata D and F.

4 TENDER PROJECT

The bidding project was developed in 2021 for the Federal Investment Council (CFI), a federal public agency for innovation and investment planning for the integral development of Argentina.

It was proposed in two distinct stages to address the urgent situation of the Molino Blanco bridge in the initial stage and to mitigate the erosive impact of water on the waterfall. The second stage involves a long-term solution to limit the waterfall's retreat in relation to the bridge.

4.1 *Stage I*

The design involves reinforcing the foundation of the Molino Blanco bridge by incorporating piles at deeper levels than the current ones, which are insufficient to account for the estimated erosion levels.

The bridge was reinforced by installing additional piles connected to the abutments and piers of the existing bridge, following these design considerations: bridge bed erosion of -1.0 m (IGN), design flow 1250 m^3/s, head beam dimensions of 2.20m x 2.80 m, and piles with a 1.50 m diameter and tip elevation of -12m/-16m (IGN). The complexity in this case arose from planning the execution works due to the difficulties of access and the limited working space (Figure 12).

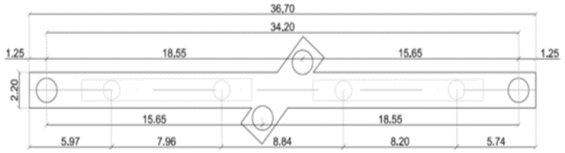

Figure 12. Linkage system between bridge structure and reinforcement piles.

The design principle applied for protecting the stream bed at the waterfall involved a combination of reducing the energy of the waterfall and improving the soil by cementing the soil layer where erosion is presumed to occurs at the foot of the waterfall.

It is planned to intervene at the waterfall by placing 1.20m concrete blocks at the foot of the waterfall up to an elevation of IGN +5.0m and to carry out a localized soil improvement of limited size through jet grouting behind the waterfall. Additionally, protection against surface erosion on the slopes of the banks and under the bridge is included. The rockfill was designed to withstand a design flow of 650 m^3/s, considering the weight limitation of the blocks. Ultimately, the modified US Army Corps of Engineers cube design was chosen, featuring a side length of 0.8m and a slope of 1V:6H (Figure 13).

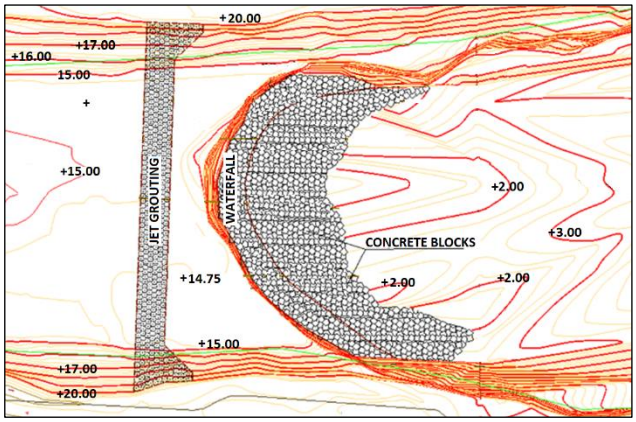

Figure 13. Plan view of stage I waterfall protection.

4.2 *Stage II*

This stage involves a solution with a cantilever structural diaphragm walls combined with jet grouting for ground improvement. The purpose is to maintain the design level in terms of passive soil resistance and to limit soil erosion up to an elevation of IGN +6.0m. This level is necessary to ensure compatibility between the chosen typology and the wall thickness with the available equipment.

The hydraulic design parameters include a design flow between 0 m^3/s to 1250 m^3/s. Table 2 summarizes the hydraulic cases analyzed for the geotechnical and structural designs. The soil bed erosion elevation is IGN -3.0m.

Table 2. Hydraulic cases analyzed for the engineering project.

Hydraulic case	*Flow* [m^3/s]	*Parana River IGN level*	*Waterfall's Downstream & Upstream River IGN level*
A1	0	+4.20	+4.0 / +15.0
A2	200	+4.20	+7.0/ +17.0
A3	200	+8.25	+8.50 / +17.0
A4	650	+4.20/+8.25	+10.0/ +17.50
A5	800	+4.20/+8.25	+11.0 / +18.0
A6	1250	+4.20/+8.25	+12.50 / +19.0
A7	1250	+4.20/+8.25	+13.50 / +20.0

The diaphragm cast wall has a curved configuration, is 1.20m thick, and consist of modules ranging from 2.50m to 2.80m wide, joined at the upper level by a crowning beam with a cross-section of 1.50m x 1.50m. The top elevation of the wall has been set at IGN level -12.00m. Ground improvement is proposed through staggered injection at the base of the central section of the diaphragm walls. The upper injection level is set at +6.00m over a length of 30m in three staggered modules of 10m each, with lower injection levels at -10.00m, -5.00m, and -3.00m (Figure 14).

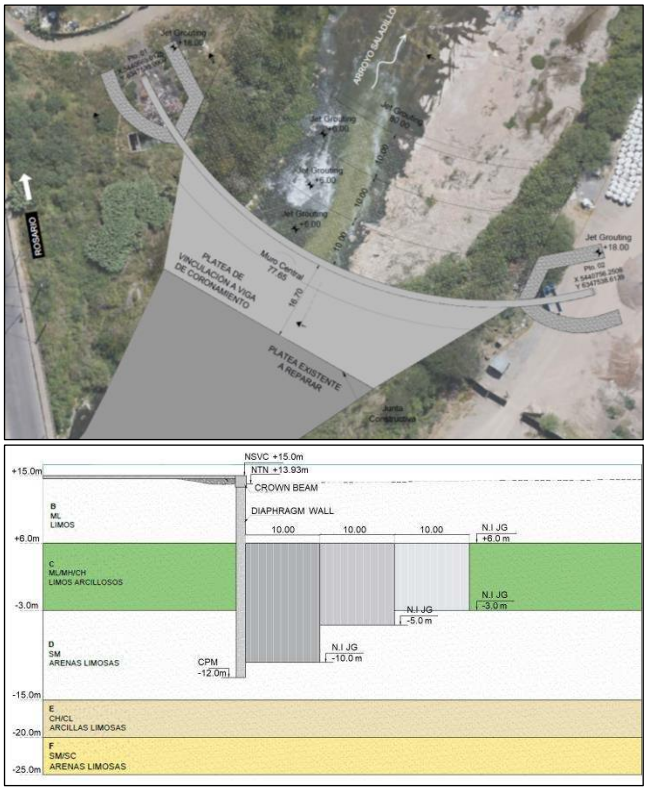

Figure 14. Tender project: diaphragm walls and jet grouting soil treatment.

5 BASIC AND DETAILED ENGINEERING DESIGN

5.1 *Redesign of tender Stage II*

At the time of awarding the work to the contractor, force majeure circumstance prevented the execution of the bidding project due to the unavailability of equipment required for soil improvement using jet grouting.

The challenge was to replace the tender project with an alternative design that avoided the massive use of jet grouting for soil improvement, instead using more structural concrete elements such as diaphragm walls and beams (items already included in the contract with unit prices) without altering the contract budget. After several conceptual analysis (including cantilever and anchored diaphragm walls) and iterations with the contractor and the client, the so called "double diaphragm walls" was chosen as the design for construction.

5.2 *Structural design*

Figure 15 shows the design of the double diaphragm walls. It consists of a continuous diaphragm wall with a thickness of 1.20m and a 2.50m long downstream module arranged in an arched configuration (radius 80m). Additionally, it includes a discontinuous diaphragm wall of 1.20m x 2.50m in a radial configuration upstream. Both diaphragm walls are spaced 28m apart, with a tip foundation at -21m (IGN), crowning beams at +14.80m (IGN), and are rigidly connected by a series of beams that are 2m wide and 1.30m/2.80m high. At both ends of the downstream diaphragm walls, the module is rotated 90 degrees to serve as an anchor for the arch. A 0.40m thick concrete slab covers the stream area to prevent soil erosion between the walls.

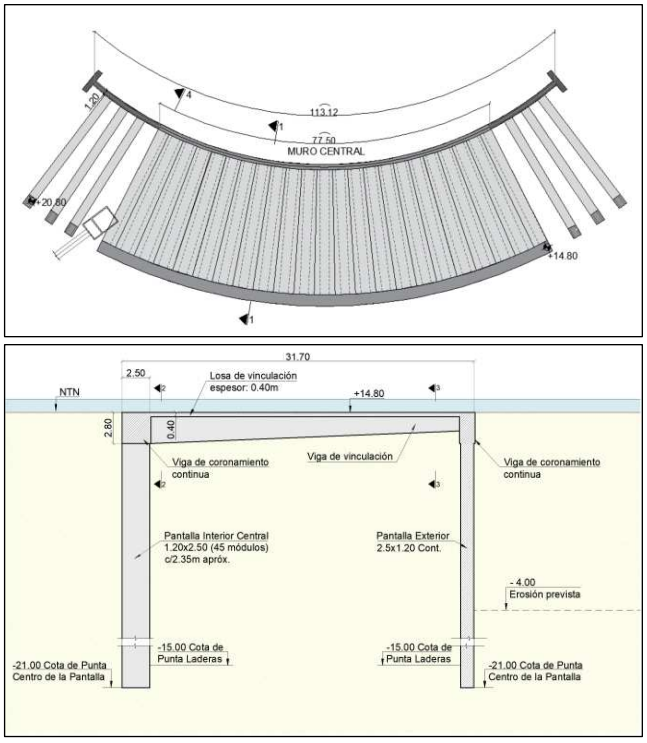

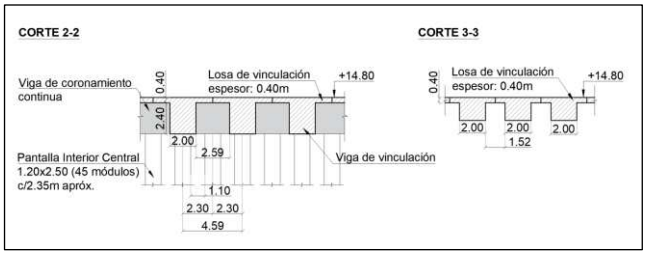

Figure 15. Basic engineering project: rigid double diaphragm walls frame.

5.3 *Geotechnical FEM 2D model*

Figure 16 presents a geotechnical bidimensional model developed using the Finite Element Method (FEM) implemented in the Plaxis software. This model was used to define the elevation of the foundation tip and the distance between the downstream and upstream diaphragm walls. The walls and beams were modeled as plate elements with a perfect elasto-plastic behavior according to their ultimate structural capacity for flexure and normal forces considering the concrete section properties as no fissured. The soil was modeled with the Hardening Soil Model (HSM) constitutive model, Mohr-Coulomb plasticity criterion and drained conditions. The undrained condition is more stable due to the high cohesion of the preconsolidated and cemented layers A, B and C, and is not as representative due to the high hydraulic permeability of these soils. The initial stress at the beginning of the analysis was considered with the K0 procedure, with K0 being the ratio between the horizontal and vertical stress in situ. The construction sequence considered for each hydraulic case was i) initial stress generation; ii) activation of the structure; iii) simulation of the hydraulic case as steady flow simultaneously with the deactivation of the downstream clusters to model the soil bed erosion; iv) Shear Strength Reduction analysis to evaluate the factor of safety. The primary goal of this model is to determine the minimum concrete steel reinforcement and the geotechnical safety factor.

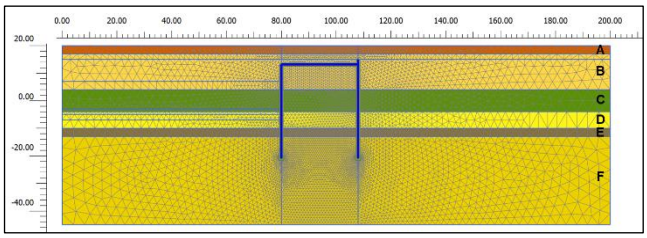

Figure 16. FEM 2D model. Mesh.

Figure 17 shows the soil displacement map for the worst-case hydraulic condition (dry season) considering the designed bed erosion level (BEL) of -4.0 (IGN). Figure 18 illustrates the envelop displacement for the downstream and upstream diaphragm walls at a soil bed erosion level of -4.0 (IGN) as the design level and -7.0 (IGN) for sensitivity analysis. The maximum displacement for the wall is 70mm at BEL -4.0 for all hydraulic case studied.

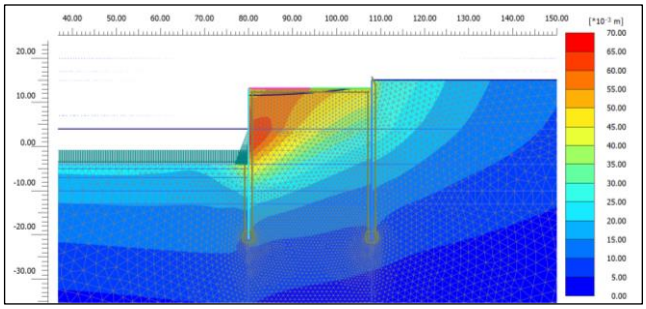

Figure 17. FEM 2D model. Total displacements. Hydraulic case: A1 - Dry season.

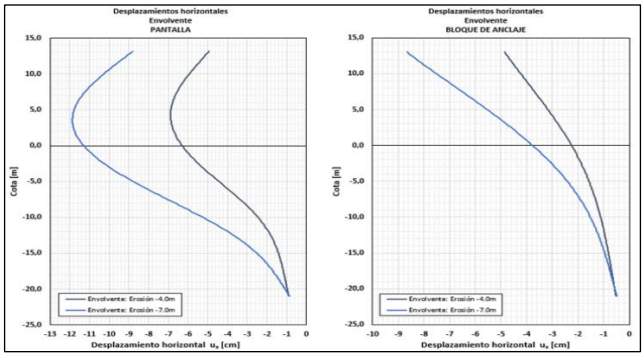

Figure 18. FEM 2D model. Displacements envelop for diaphragm walls for bed erosion levels of -4.0 and -7.0m (IGN).

Shear Strength Reduction analysis (SSR) was carried out under different hydraulic cases, ranging from a dry stream (A1) to a peak flow stream of $1500\,m^3/s$ (A7). Table 3 summarizes the achieved factors, which all exceed 1.50 for the design condition (EBL -4.0) and 1.40 for the extreme condition (EBL -7.0). Figure 19 shows the typical failure mode, showing active and passive zones on the downstream and upstream side of the continuous diaphragm walls. Examining the failure mechanism, the upstream discontinuous diaphragm walls serve as an inefficient horizontal anchor for the beams. Moving the anchor wall upstream would decrease displacements and increase the SSR, but physical constraints due to the proximity of the nearby bridge and budget constraints due to cost overruns (longer beams) led to the adoption of a compromise measure.

Table 3. Shear Strength Reduction factors for three erosional bed levels (EBL) for each hydraulic case (stream flow in m^3/s, Parana River Level).

Hydraulic case	*-4.0*	*-5.0*	*-7.0*
A1 – dry season	1.78	1.66	1.47
A2 (200, +4.20 IGN)	1.81	1.68	1.50
A3 (200, +8.25 IGN)	1.90	1.79	1.57
A4 (650, +4.20 or +8.25 IGN)	1.99	1.87	1.66
A5 (800, +4.20 or +8.25 IGN)	2.04	1.91	1.69
A6 (1250, +4.20 or +8.25 IGN)	2.08	1.96	1.74
A7 (1500, +4.20 or +8.25 IGN)	2.08	1.97	1.74

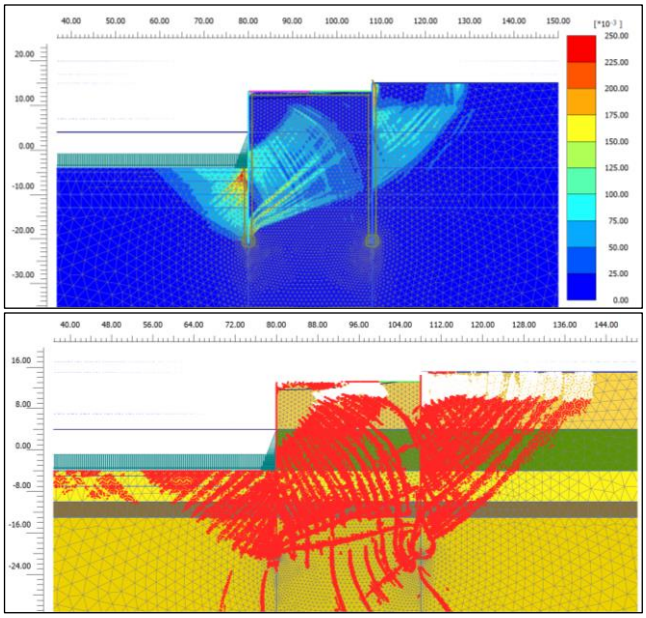

Figure 19. FEM 2D SSR phase. Case A-1. Deviatoric strain. Plastic points.

Figure 20 shows the ultimate bending moments envelope of the SSR analysis (solid line), and service load cases (dotted line) multiplied by 2.20 for EBL -4.0 (black line) and EBL -7.0 (blue line). The factor of 2.20 is the load factor for hydraulic structures (EM 1110-2-2104 *Strength Design for Reinforced-Concrete Hydraulic*). The steel reinforcement adopted for both concrete walls covers both envelopes.

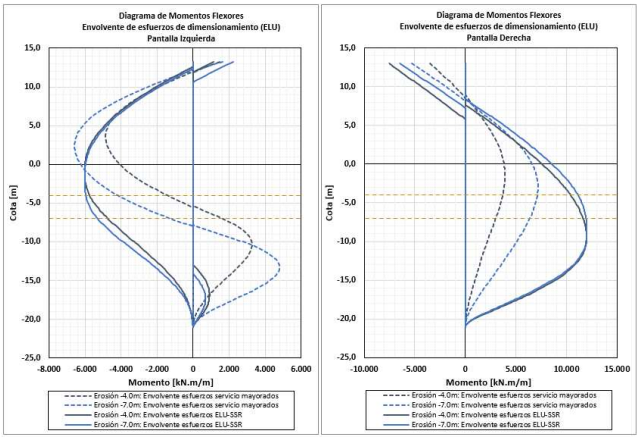

Figure 20. FEM 2D model. Ultimate bending moments envelop.

5.4 *Geotechnical FEM 3D model*

The main objective of this model is to assess the beneficial effect of arched arrangement of the diaphragm walls, obtain a more accurate estimate of displacements, and capture behaviors that only a 3D model can represent. Figure 21 shows detail of the mesh, structure, and phases (initial in situ stress, initial excavation, structure activation, soil erosion downstream, hydraulic condition for case A1 and A7). Vertical joints between modules on the downstream wall could not be modeled due to software limitations, leading to an undesirable overestimation of the wall's flexural rigidity, which may result in underestimation of displacements.

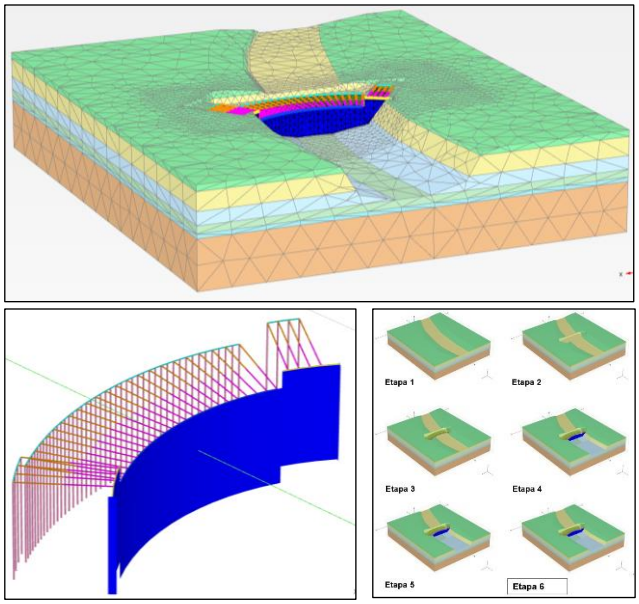

Figure 21. FEM 3D model. Mesh. Structural plates and beams. Phases.

For the hydraulic case A1, Figure 22 shows total displacement (max. 36mm), horizontal axial forces (max. 7000 kN/m) and vertical moments (max. 1500 kNm/m). The ratio between 3D and 2D models for the maximum horizontal displacement of the wall is 0.50, and for maximum vertical moment is 0.65. This confirms that the arched arrangement is effective in controlling displacement and provides an additional safety margin for this complex and unusual structure, as it relies on the local effectiveness of the supporting soil at the ends of the arch.

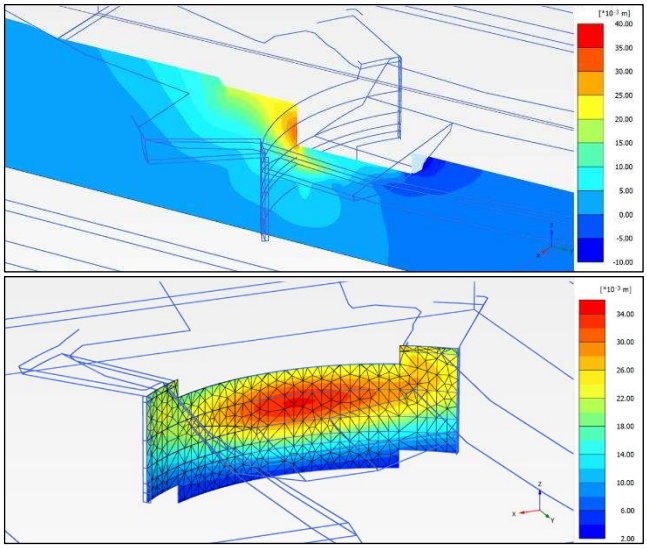

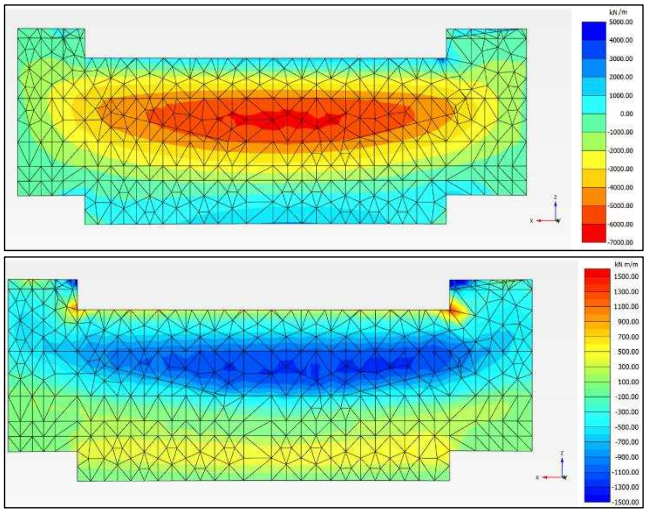

Figure 22. FEM 3D. Case A1. Longitudinal and total displacements [mm]. Horizontal axial forces [kN/m]. Vertical moments [kNm/m].

An analysis of the overall behavior of the structure reveals that the concrete slab on the surface, which is attached to the beams, forces the entire structure to shift in the direction of the river axis (stream direction). The discontinuous upstream diaphragm walls consist of isolated modules measuring 1.20m x 2.50m, with weak axes oriented in the radial direction of the arch. The 2D models predict bending moments only in the strong axis of each module, but the full 3D model reveals bending moments in the weak axis as well (Fig. 23) because soil reaction occurs along the long side of the module. This effect intensifies as the modules move farther from the center of the river due to the increasing angle between the radial direction of the beams and the stream's direction. To accommodate this structural demand, additional steel reinforcements were added along the long sides of the modules. The 3D model proved to be a suitable tool to verify the 2D models used in the previous design stages and understand global behavior that cannot be fully captured with these models.

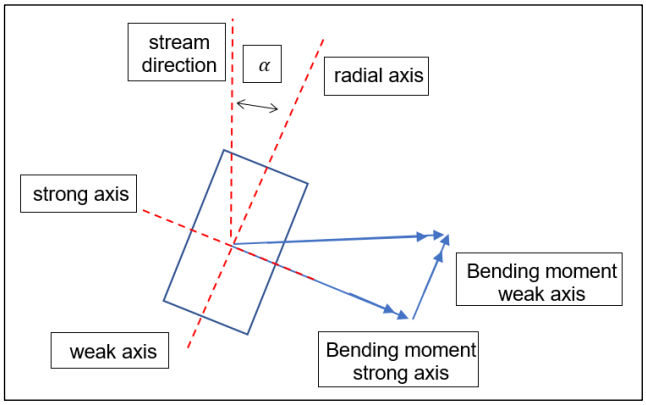

Figure 23. Isolated module of the discontinuous upstream diaphragm walls.

5.5 *Calibration of a spring structural model*

Since not all design loads are accounted for in the geotechnical models, a structural model incorporating all service and ultimate loads, along with their combinations as specified in CIRSOC 201 and ACI318 (e.g., temperature changes, shrinkage, seismic loads, cracking, etc.), is used to design the steel reinforcement of the concrete structure. The challenge arises in determining how to consider the loads and moduli of soil reaction on a structure composed of two diaphragm walls that interact with each other.

The pressures on each side of the diaphragm walls and beneath the beams were interpreted based on the results from the 2D geotechnical model. An interactive process was conducted, in which loads were defined through analytical analysis (including passive or active pressures) and fixed pressure values (Fig. 24) for each hydraulic case (A1 to A7). These pressures were combined with horizontal and frictional elastic spring values, or soil reaction moduli (Fig. 25), to align the structural forces between the structural and geotechnical models (Fig. 26), prioritizing the calibration of bending moments before normal forces.

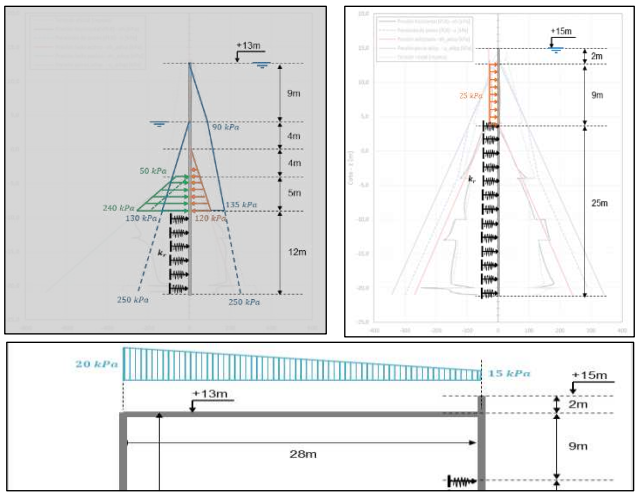

si

Figure 24. Loads for soil and water and springs defined for the downstream and upstream walls and beam at service loads for hydraulic case A1. At background, pressures result from geotechnical model.

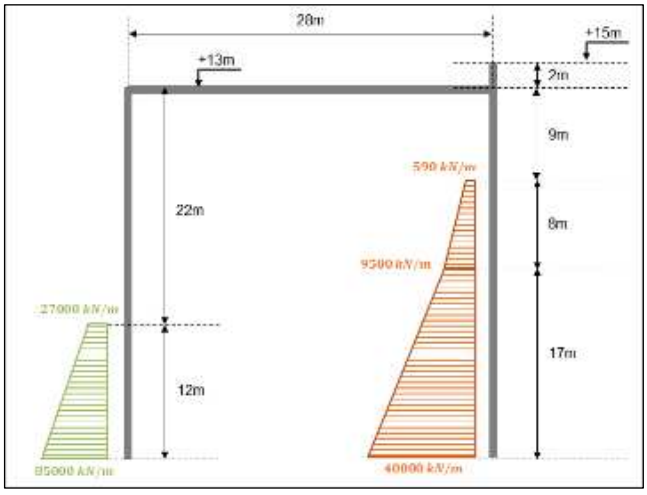

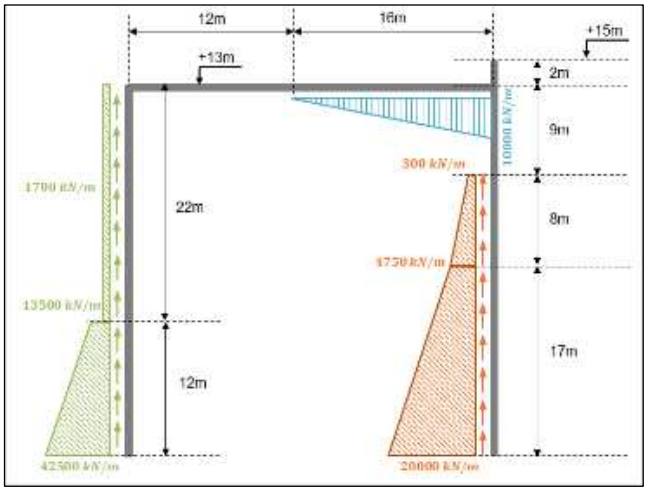

Figure 25. Horizontal and Vertical reaction modulus to simulate the soil in the spring structural model under service loads.

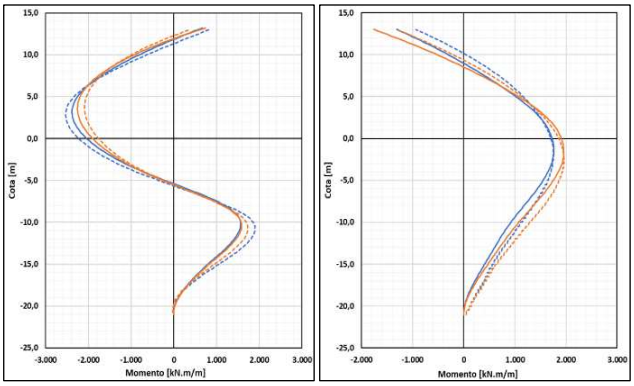

Figure 26. Bending moment for structural (dotted) and geotechnical FEM 2D (continuous) model for hydraulic case A1 (blue) and A7 (red), for downstream (left) and upstream (right) diaphragm walls.

6 CONCLUSIONS

A solution to address the retrogressive erosion problem at the Saladillo Waterfall was proposed. Limitation regarding the availability of jet grouting equipment during construction compromised the feasibility of the tender project. Consequently, the "double diaphragm walls" design was proposed to meet the program's budget and scheduling requirements. The structural solution is intricate and unprecedented, with no similar cases found worldwide. Extensive geotechnical analyses were conducted to thoroughly understand the structure's interaction with the soil and to minimize any undesirable effects.

7 REFERENCES

Basile, P. & Riccardi, G., 2017, Modelación morfodinámica del proceso de erosión retrogradante: Aplicación a la cascada del Aº Saladillo, Actas VII Simposio regional sobre hidráulica de ríos.

EM 1110-2-2104, 2016. Strength Design for Reinforced-Concrete Hydraulic.

Kondner, R.L. 1963. "Hyperbolic Stress-Strain Response: Cohesive Soils", Journal of the Soil Mechanics and Foundations Division, ASCE, Vol. 89, No. SM1, Feb, p. 115.

Parent, et al., 2010. Estratigrafía del cuatenario del sur de la provincia de Santa Fe, Argentina, Boletín del Instituto de Fisiografía y Geología 72-75, Rosario, ISSN 1666-115X, pp: 47-54.

Pasotti, P., 1982. La Neotectónica en el área del Gran Rosario, Provincia de Santa Fe, Argentina. Actas Quinto Congreso Latinoamericano de Geología 1, Buenos Aires.

Schanz, T. & Vermeer, P.A., 1998. On the stiffness of sands, Géotechnique 48, 383-387.

Sosa, V. et al, 2012, Análisis de la variabilidad espacial del peso unitario seco en un sector céntrico de la ciudad de Rosario. Uso de técnicas geoestadísticas, Actas XXI Congreso Argentino de Mecánica de Suelos e Ingeniería Geotécnica, Conferencias y resúmenes de la selección de trabajos, 149.

Yrigoyen, M. 1975. Geología del subsuelo y plataforma continental. Geología y Recursos Naturales de la provincia de Buenos Aires. 6º Congreso Geológico Argentino (Bahía Blanca), Relatorio: 139-168, Buenos Aires.